HIGH ENERGY γ-RAY EMISSION IN HEAVY-ION COLLISIONS*

W. BAUER[1], W. CASSING, U. MOSEL and M. TOHYAMA

Institut für Theoretische Physik, Universität Giessen, 6300 Giessen, West Germany

R.Y. CUSSON

GSI Darmstadt and Physics Department, Duke University, Durham N.C. 27706, USA

Abstract: We calculate double-differential cross sections for energetic photon production in intermediate energy nucleus–nucleus collisions. The production mechanism is assumed to be either that of collective bremsstrahlung or that of electromagnetic transitions between time-dependent single-particle states as emerging from a self-consistent treatment of the heavy-ion dynamics in the one-body limit (TDHF). Effects from residual nucleon–nucleon collisions on the collective current are further taken into account via a relaxation ansatz for the single-particle occupation numbers. The total yields for energetic photon production above 50 MeV in the simple limit considered indicate that up to 10% of the experimental cross sections can be attributed to collective bremsstrahlung and electromagnetic transitions.

1. Introduction

High energy photon emission in heavy-ion collisions has recently gained interest since it provides an additional probe for the heavy-ion dynamics apart from energetic light particles or pions. A variety of models have been developed in the last years ranging from collective bremsstrahlung [1-3] to "statistical treatments" of the A-body problem [4]. Emission from a hot spot and production by nucleon–nucleon bremsstrahlung have been considered as well [5]. Most of these approaches, however, lack a more microscopic foundation on the underlying heavy-ion dynamics and their range of validity should be determined by parameter-free calculations. In this paper we aim at solving the latter problem with respect to bremsstrahlung.

We outline the general framework in sect. 2 and derive the expressions for the double differential cross section in the one-body limit. A detailed evaluation of the γ-yield is performed in slab on slab geometry for $^{12}C + ^{12}C$ at laboratory energies from 84 to 160 MeV/u. Results of explorative calculations within three-dimensional TDHF dynamics are presented in sect. 3 for $^{16}O + ^{16}O$ at 80 MeV/u laboratory energy.

The effect of residual nucleon–nucleon collisions on collective photon bremsstrah-lung is investigated additionally within the modified relaxation approach of Tohyama [6]). A summary of the present results as well as a future outlook is given in sect. 4.

2. General formulation

We consider the interaction density

$$H^{int} = j_\mu A^\mu , \qquad (2.1)$$

between the nuclear electromagnetic current j_μ and the electromagnetic field A_μ within Heaviside–Lorentz units. The S-matrix for this hamiltonian density is given in first order perturbation theory by

$$S = 1 - i \int d^4x \, j_\mu A^\mu , \qquad (2.2)$$

where the operators are described in the interaction picture.

The number of photons in the interval $[k, k + \Delta k]$ is given by

$$\frac{dn}{dk^3} = \sum_\lambda \sum_f \left| \int \langle \hat{k}, \lambda \| \langle \psi_f | j_\mu A^\mu | \psi_i \rangle \| 0 \rangle \, d^4x \right|^2 , \qquad (2.3)$$

where ψ_i and ψ_f denote the initial and final states of the nuclear system while $\| 0 \rangle$ denotes a zero-photon state and $\| \hat{k}, \lambda \rangle$ a single-photon state with photon 4-vector $\hat{k}$ and polarization λ.

The restriction to single-photon states in (2.3) should be justified in the intermedi-ate energy domain from roughly $20 \, \text{MeV}/u$ to $160 \, \text{MeV}/u$ because the coupling constant of the electromagnetic interaction is small.

In the radiation gauge eq. (2.3) may be written in the form

$$\frac{dn}{dk^3} = \frac{1}{2\omega} \sum_f \sum_\lambda (2\pi)^{-3} \left| \int d^4x \, e^{i\hat{k}\cdot\hat{x}} \langle \psi_f | \boldsymbol{j} \cdot \boldsymbol{\varepsilon}(\hat{k}, \lambda) | \psi_i \rangle \right|^2 , \qquad (2.4)$$

where $\boldsymbol{\varepsilon}(\hat{k}, \lambda)$ is a unit polarization vector corresponding to a photon with $(\hat{k}, \lambda)$. The two polarization vectors $\boldsymbol{\varepsilon}(\hat{k}, \lambda_1)$ and $\boldsymbol{\varepsilon}(\hat{k}, \lambda_2)$ are orthogonal to $k/|k|$, which implies that photons only probe the transverse component of the nuclear current.

2.1. TDHF FORMALISM

Neglecting all correlations between nucleons in eq. (2.4) except those induced by the mean-field and the Pauli principle, we may replace the states ψ_i and ψ_f in (2.4) by Slater determinants. We determine the time dependence of these Slater determinants by means of the TDHF method. In this way we retain the collective

stopping of the two nuclei by the mean-field and treat the important energy-momentum correlation in the single-particle (s.p.) states. Furthermore, we include dynamical distortions both in x- and in p-space and treat the Pauli principle exactly.

We note that this method has led to quite realistic results for the pion production in heavy-ion reactions [7]).

In addition to the s.p. limit for the states ψ_i and ψ_j we restrict to the s.p. limit of the current which in the nonrelativistic limit is given by [8])

$$j_q = -\frac{ie}{2m}(1+\tau_3)(\varphi^+\nabla\varphi - \varphi\nabla\varphi^+) + \mu_q\nabla\times(\varphi^+\boldsymbol{\sigma}\varphi),\tag{2.5}$$

where φ is a nucleon field operator. The first part represents the "Schrödinger"-convection current and the second part the spin current. The magnetic moments are given by

$$\mu_p = 2.79\mu_k = 2.79\frac{e}{2m},$$

$$\mu_n = -1.91\mu_k.\tag{2.6}$$

The final expression for the matrix elements of the current operator in eq. (2.4) is

$$j_{ij}^p = -\frac{ie}{2m}(\varphi_{jp}^*\nabla\varphi_{ip} - \varphi_{ip}\nabla\varphi_{jp}^*) + \mu_p\nabla\times(\varphi_{jp}^*\boldsymbol{\sigma}\varphi_{ip})\tag{2.7}$$

for protons and

$$j_{ij}^n = \mu_n\nabla\times(\varphi_{jn}^*\boldsymbol{\sigma}\varphi_{in})\tag{2.8}$$

for neutrons where φ_i are time-dependent s.p. states building up the Slater determinants ψ_i and ψ_f in (2.4). From eq. (2.8) we see that neutrons have a nonvanishing contribution to the photon yield which will become important at higher photon energies (cf. sect. 3). The number of photons in the interval $[k, k+\Delta k]$ is then given by

$$\frac{dn}{dk^3} = \frac{(2\pi)^{-3}}{2\omega}\sum_\lambda\left|\sum_h\int d^4x\,e^{ik\cdot\hat{x}}j_{hh}\cdot\boldsymbol{\varepsilon}(\hat{k},\lambda)\right|^2$$

$$+\frac{(2\pi)^{-3}}{2\omega}\sum_\lambda\sum_{p,h}\left|\int d^4x\,e^{ik\cdot\hat{x}}j_{ph}\cdot\boldsymbol{\varepsilon}(\hat{k},\lambda)\right|^2,\tag{2.9}$$

where the sums over p and h run over particle- and hole-states, respectively.

The first part of eq. (2.9) describes the photon production via the space and time variation of the one-body current (collective bremsstrahlung); the second part gives in addition the yield due to electromagnetic transitions between occupied and unoccupied time-dependent s.p. states during the collective deceleration.

The total yield of photons per solid angle $d\Omega$ in the interval $(\omega, \omega+\Delta\omega)$ is finally given by an integral over impact parameter b using $d^3k = \omega^2\,d\omega\,d\Omega$, because the

currents j_{ph} and j_{hh} in eq. (2.9) also depend on the impact parameter b of the nucleus–nucleus collision, i.e.

$$\frac{d^2\sigma}{d\omega\, d\Omega} = \omega^2 \int_0^\infty \frac{dn(b)}{dk^3}\, d^2b.$$ (2.10)

Apart from the solution of the time-dependent Hartree–Fock problem for fixed b with respect to occupied and unoccupied s.p. states, the evaluation of eq. (2.9) requires a four-dimensional Fourier integration for a large number of different Slater-determinants ψ_{ph}. We thus will restrict our studies to a few explorative unrestricted 3-dimensional calculations and use a simpler geometry for more systematic studies.

2.2. SLAB GEOMETRY

In this section we restrict ourselves to slab geometry, i.e. we assume that the s.p. wavefunctions perpendicular to the beam (z-) direction may be approximated by plane waves such that part of the integrals in eq. (2.9) can be carried out analytically.

Originally this approach was proposed by Bonche, Koonin and Negele[9] and in the intermediate energy regime has been quite successfully applied to pion production[7].

In detail: the s.p. wavefunctions are

$$\psi_{nk_\perp}(\mathbf{r}, \sigma, \tau, t) = T(\tau)S(\sigma)\psi_{nk_\perp}(\mathbf{r}, t),$$ (2.11)

where σ and τ represent spin and isospin coordinates, respectively, and the spatial part of the wave function is given by

$$\psi_{nk_\perp}(\mathbf{r}, t) = \frac{1}{\sqrt{\Omega}} \exp\left[-ik_\perp^2 t/2m\right]\varphi_n(z, t)\, e^{ik_\perp \cdot r_\perp}.$$ (2.12)

Here Ω is a two-dimensional normalization volume. The time-evolution of $\varphi_n(z, t)$ is determined by TDHF. From this point on it is straightforward to perform the following steps:

(a) Calculate the matrix elements of the current density operator between the two Slater determinants representing the initial and final states in eq. (2.9);

(b) perform the projection of these matrix elements onto the transverse components;

(c) perform the Fourier transformation to obtain dn/d^3k.

The final result is[10]

$$\begin{aligned}
\frac{dn}{dk^3} = &\frac{1}{\omega}\frac{\Omega}{(2\pi)^5}\frac{e^2}{2m^2}\sum_{\varepsilon_p\varepsilon_h}\int\int\Big[\{2(k_z^2 + k_x^2)(\mu_p^2 + \mu_n^2)\\
&+ [k_z^2/(k_x^2 + k_z^2)](2k_x^h - k_x)^2 + (2k_y^h)^2\}|I_1|^2\\
&+ [k_x^2/(k_x^2 + k_z^2)]|I_3|^2 - [k_xk_z/(k_x^2 + k_z^2)](I_1^*I_3 + I_1I_3^*)]\\
&\times \Theta_w(|k_\perp^h - k_\perp| - r_p)\, d\,k_x^h dk_y^h,
\end{aligned}$$ (2.13)

with

$$\Theta_{\mathrm{w}}(|k_\perp^h - k_\perp| - r_p) = \begin{cases} 1 & \text{for } \varepsilon_p > \varepsilon_{\mathrm{F}} \\ \Theta(|k_\perp^h - k_\perp| - r_p) & \text{for } \varepsilon_p \leqslant \varepsilon_{\mathrm{F}} \end{cases}$$

$$r_p = (2m(\varepsilon_{\mathrm{F}} - \varepsilon_p))^{1/2}.$$

We have assumed spin–isospin saturation to obtain this expression. The photon unit vector is represented by

$$\boldsymbol{e}_k = (k_x, 0, k_z)/(k_x^2 + k_z^2)^{1/2}. \tag{2.14}$$

We ensure that $\boldsymbol{e}_k$ always has a vanishing y-component by a proper choice of the coordinate system, thus using the azimuthal symmetry of the problem. The summation over ε_h extends over all states with asymptotic s.p. energies ε_n below the Fermi energy ε_{F}, whereas ε_p indicates a summation over all unoccupied states.

We discretize the states above the Fermi energy as described in ref. [7]. For slab on slab collisions corresponding to the system $^{12}C + {}^{12}C$ at lab energies up to 160 MeV/u we find numerically, that it is sufficient to include the first 10 unoccupied states in eq. (2.13).

The integration over k_x^h and k_y^h, which represent the two perpendicular components of the hole–state wave vector, extends over a circle with radius

$$r_h = (2m(\varepsilon_{\mathrm{F}} - \varepsilon_h))^{1/2}. \tag{2.15}$$

Finally, the integrals I_1 and I_3 appearing in (2.13) are given by

$$I_1 = \int \int \varphi_p^*(z, t)\varphi_h(z, t) \exp(-ik_z z) \exp\{it(\omega - (2k_x^h k_x - k_x^2)/2m)\} \, \mathrm{d}t \, \mathrm{d}z,$$

$$I_3 = \int \int \left\{ \varphi_h(z, t) \frac{\partial}{\partial z} \varphi_p^*(z, t) - \varphi_p^*(z, t) \frac{\partial}{\partial z} \varphi_h(z, t) \right\} \exp(-ik_z z)$$

$$\times \exp\{it(\omega - (2k_x^h k_x - k_x^2)/2m)\} \, \mathrm{d}t \, \mathrm{d}z \tag{2.16}$$

and evaluated numerically as described in ref. [10]. As may be seen from eq. (2.13), there is no contribution from diagonal matrix elements to the photon yield in the slab geometry. This results from the use of momentum eigenstates in transverse direction and the transversality of the photon. The "bremsstrahlungs" component is thus missing in the slab calculations. One could try to correct this shortcoming of the slab geometry by cutting the slab in the transverse direction to a length of the order of the nuclear diameter. The spectrum of the photons would then, however, still be undetermined.

The expression in eq. (2.13) is the number of photons emitted per unit area of the slabs. A cross section is obtained by approximating the colliding nuclei by cylinders in coordinate space. The overlap of these cylinders for a given impact parameter b is [10]

$$S(b) = 2R^2 \arccos(b/2R) - b(R^2 - \tfrac{1}{4}b^2)^{1/2}. \tag{2.17}$$

An integration over impact parameter then yields

$$\frac{\mathrm{d}\sigma}{\mathrm{d}^3 k} = R^4 \pi^2 \frac{\mathrm{d}N}{\mathrm{d}^3 k} \frac{1}{\Omega},$$

$$(2.18)$$

where Ω is the normalization volume as in (2.13).

3. Numerical results

The evaluation of the double differential cross section $\mathrm{d}^2\sigma/\mathrm{d}\omega\,\mathrm{d}\Omega$ is uniquely defined by eqs. (2.9) and (2.10) and in principle can be carried out without further approximations. The numerical evaluation of eq. (2.9), however, is quite time consuming; we, therefore, reduce the problem by a few suitable approximations that do not affect the physical significance of the results. In this spirit we first discuss the results of a calculation in the one-dimensional slab geometry. In this framework we can perform exploratory studies of many different physical observables, like the γ-spectra, their bombarding energy dependence and their angular distribution.

3.1. SLAB ON SLAB COLLISIONS

The particular assumptions concerning the slab geometry have been presented in sect. 2.2 and the evaluation of the double differential cross section (2.18) along the line of eqs. (2.13) to (2.16) is still cumbersome but straightforward. The large sum over all p-h matrix elements can be carried out without major difficulties. The slab calculations are expected to yield valuable information on the contributions of the nondiagonal terms in eq. (2.9) that have so far not been considered in the literature.

Fig. 1 shows the result of such a calculation; the full line displays the double differential γ-cross section at 90° for ^{12}C + ^{12}C at 84 MeV/u. It is seen that the spectrum is clearly steeper than the experimental data [from ref. [11]] indicated by open circles in the figure. In addition the absolute yield is too low by about an order of magnitude. The question whether these discrepancies are due to the restricted geometry, due to a shortcoming in the TDHF dynamics or due to an improper treatment of the elementary vertex has to be left open at this point. We will return to these questions in the next section.

In fig. 2 we show the angular distribution for photons of 50 MeV, 100 MeV and 150 MeV energy in the c.m. system (full lines) which according to eqs. (2.7) and (2.8) may be decomposed into contributions from the convection current (dash-dotted lines), the spin current of protons (dotted lines) and the spin current of neutrons (dashed lines). The system studied corresponds to ^{12}C + ^{12}C at 84 MeV/u. According to the interference between spin and convection currents [cf. eqs. (2.7) and (2.9)] the total angular distribution (full lines) is not simply the sum of the various contributions. At all photon energies the contribution from the convection current dominates which is essentially of dipole shape in the c.m. system. The
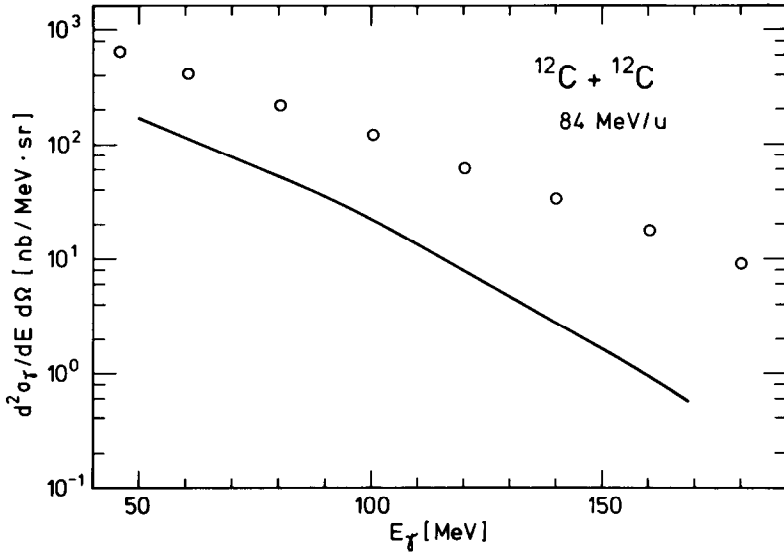
Fig. 1. The double differential photon yield $d^2\sigma_\gamma/dE\,d\Omega$ as emerging from electromagnetic transitions for $^{12}C + {}^{12}C$ at 84 MeV/u in slab geometry for $\vartheta_\gamma = 90°$. The open circles denote experimental data at $\vartheta_\gamma = 90°$ in the nucleus–nucleus c.m. system for the same reaction [from ref. [11]].
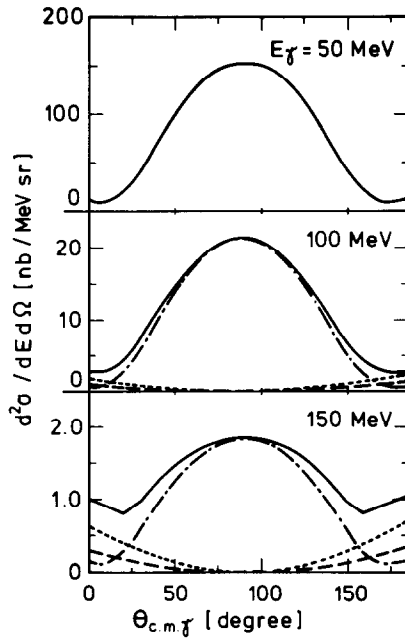

Fig. 2. Angular distribution of energetic photons ($E_\gamma = 50$ MeV, 100 MeV and 150 MeV) in the c.m. system for $^{12}C + {}^{12}C$ at 84 MeV/u as evaluated in slab geometry (full lines). The relative contributions from the convection current, spin current of protons and spin current of neutrons are displayed in terms of the dash-dotted, dotted and dashed lines, respectively.

influence of the spin currents is only significant at very high photon energies and forward (backward) angles filling up the minimum from the convection current.

Angle integrated photon yields are displayed in fig. 3 for $E_\gamma = 50$ MeV and $E_\gamma = 150$ MeV as a function of the laboratory energy per nucleon E/A. The double logarithmic plot suggests a parametrization of the form

$$\frac{d\sigma}{dE_\gamma} \sim (E/A)^x ,\tag{3.1}$$

which yields $x = 0.95$ for $E_\gamma = 50$ MeV and $x = 3.3$ for $E_\gamma = 150$ MeV (straight lines in fig. 3) in rough agreement with the experimental observation [12]). The different scaling behaviour for small and high energy photons is due to the fact that energetic γ-rays probe the high momentum tail of the nuclear momentum distribution which varies drastically with bombarding energy.

The total photon yield above 50 MeV for $^{12}C + ^{12}C$ at 84 MeV/u in the slab geometry is 35 μb which accounts for roughly 20% of the experimental yield $(160 \pm 34 \ \mu b)$ [11]).
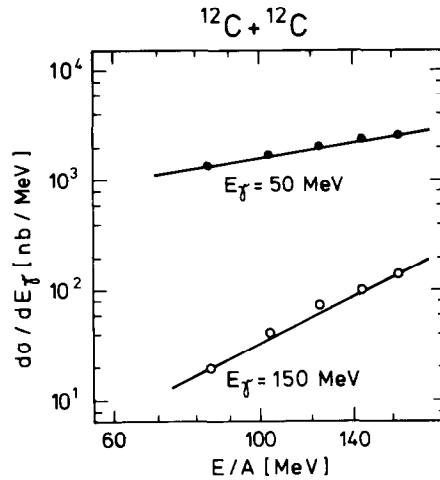

Fig. 3. The angle-integrated photon yield for $E_\gamma = 50$ MeV and $E_\gamma = 150$ MeV from $^{12}C + ^{12}C$ as a function of the laboratory energy per nucleon. The straight lines express the scaling behaviour (3.1).

3.2. THE THREE-DIMENSIONAL PROBLEM

As a first step we replace the integral over impact parameter in eq. (2.10) by the double differential photon multiplicity $dn(\bar{b})/dk^3$ at an average impact parameter $\bar{b}$ and multiply by the geometrical cross section, i.e.

$$\frac{d^2\sigma}{d\omega \, d\Omega} = \omega^2 \frac{dn(\bar{b})}{dk^3} \times \pi r_0^2 A^{2/3} ,\tag{3.2}$$

where A denotes the mass-number of the target or projectile in case of symmetric collisions. The radius parameter r_0 in (3.2) is assumed to be $r_0 \approx 1.2$ fm. This approximation separates the more trivial geometrical aspects of heavy-ion collisions at high energy from the elementary production mechanism invoked in eq. (2.9). We concentrate on the system $^{16}O + ^{16}O$ at 80 MeV/u laboratory energy and adopt $\bar{b} = 1.5$ fm as an average impact parameter.

The differential photon multiplicity due to collective bremsstrahlung, i.e. the first part of eq. (2.9) then may be written as

$$\frac{\mathrm{d}n^0}{\mathrm{d}k^3} = \frac{1}{2\omega} |j_\perp(\hat{k})|^2 , \tag{3.3}$$

where $j_\perp(\hat{k})$ denotes the Fourier transform of the nuclear current $j(r, t)$ projected onto the plane orthogonal to the photon vector k:

$$j_\perp(\hat{k}) = (2\pi)^{-3/2} \int \mathrm{d}^4x \, \mathrm{e}^{ik\cdot\hat{x}} j_\perp(\hat{x}) . \tag{3.4}$$

In eq. (3.3) we have used the identity

$$\sum_{\lambda=1}^{2} |j(\hat{k}, \lambda)|^2 = \left| \sum_{\lambda=1}^{2} \varepsilon(\hat{k}, \lambda) \cdot j(\hat{k}) \right|^2$$

$$= |j(\hat{k}) - (e_k j(\hat{k}))e_k|^2$$

$$=: |j_\perp(\hat{k})|^2 , \tag{3.5}$$

since $\varepsilon(\hat{k}, \lambda_1)$, $\varepsilon(\hat{k}, \lambda_2)$ and $e_k = k/|k|$ form an orthogonal basis in coordinate space. For a spin- and isospin-saturated system the spin current drops out in eq. (3.3) such that $j(\hat{x})$ is simply given by

$$j(\hat{x}) = \frac{-ie}{2m} \sum_{\mathrm{p}} [\varphi_\mathrm{p}^* \nabla \varphi_\mathrm{p} - \varphi_\mathrm{p} \nabla \varphi_\mathrm{p}^*] , \tag{3.6}$$

where the sum runs over occupied proton s.p. states only. In this respect the evaluation of (3.3) is straightforward once the time-dependent s.p. states $\varphi_\mathrm{p}(r, t)$ have been produced by a TDHF calculation [13]).

A problem arises with respect to the Fourier transformation in time which induces a numerical uncertainty due to the finite time interval considered. Averaging over initial and final time intervals as described in detail in ref. [10]), we obtain a reasonable estimate of the γ-cross section $\mathrm{d}^2\sigma_\gamma/\mathrm{d}E \, \mathrm{d}\Omega$, which is displayed in fig. 4 in terms of the full lines at 5°, 45° and 85° in the reaction plane with respect to the beam axis. Though only three angles are considered (in the nucleus–nucleus c.m. system), the results indicate a dominant quadrupole-type distribution as expected from the interference pattern of two decelerated equal charge distributions [14]). The numerical uncertainty due to the finiteness of the time interval is displayed in terms of the vertical lines for the photon yield at 45° and is of the same order of magnitude for the other angles.
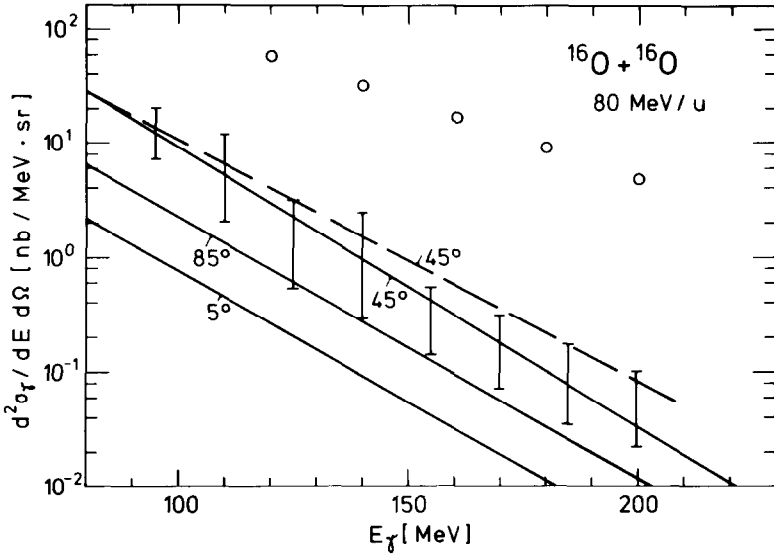
Fig. 4. The double differential photon cross section for $^{16}O + ^{16}O$ at 80 MeV/u as resulting from collective bremsstrahlung (full lines) at $\vartheta_\gamma = 5°$, $45°$ and $85°$ in the c.m. system. The numerical uncertainty is indicated by the vertical error bars at $45°$. The dashed line represents the corresponding result of the collective bremsstrahlung at $45°$, in which effects from residual nucleon–nucleon collisions on the nuclear current are taken into account. The experimental data (open circles) are the same as in fig. 1.

How do these results compare with experiment? First of all, experimental angular distributions turn out to be rather flat in the nucleon–nucleon c.m. system in contrast to a quadrupole distribution for collective bremsstrahlung [11]). In addition, the experimental photon yield (open circles in fig. 4) for $^{12}C + ^{12}C$ at 84 MeV/u and 90°, a system which should be roughly comparable to the present calculation, is at least about an order of magnitude larger. Furthermore, the inverse slope of the calculated spectrum is significantly smaller than that of the data.

One might argue that the collective deceleration by the mean-field in the one-body limit *a priori* is expected to be too small at these bombarding energies since residual two-body collisions have been neglected. In order to study the effect of residual nucleon–nucleon interactions on the collective current, calculations have been performed within the extended TDHF approach of Tohyama [6]) where the one-body occupation matrix no longer is diagonal,

$$\rho(x, x') = \sum_{\lambda,\lambda'} n_{\lambda\lambda'} \varphi_\lambda(x) \varphi_{\lambda'}^*(x') , \qquad (3.7)$$

and the occupation matrix elements are assumed to follow a relaxation equation

$$\frac{\mathrm{d}}{\mathrm{d}t} n_{\lambda\lambda'}(t) = -\frac{1}{\tau} \left(n_{\lambda\lambda'}(t) - \bar{n}_{\lambda\lambda'}(t) \right) , \qquad (3.8)$$

expressing the approach to equilibrium on a characteristic time scale τ. In eq. (3.8)

the equilibrium matrix elements are given by [6])

$$\bar{n}_{\lambda\lambda'}(t) = \sum_{\alpha} U_{\lambda\alpha}(t)\{1 + \exp((\varepsilon_{\alpha} - \mu)/T)\}^{-1}U^+_{\alpha\lambda'}(t) , \qquad (3.9)$$

where μ and T are fixed by particle–number and energy conservation, while $U_{\lambda\alpha}(t)$ is a unitary matrix diagonalizing the s.p. hamiltonian $\varepsilon_{\lambda\lambda'} = \langle\varphi_{\lambda}|h(t)|\varphi_{\lambda'}\rangle$ at each time step. The sum over α in (3.9) includes all eigenstates of h. Via eq. (3.7) additional damping of the relative motion of two colliding heavy ions is achieved which has to be attributed to residual nucleon–nucleon collisions.

The calculations were performed for $^{16}O + ^{16}O$ at 80 MeV/u; a very short relaxation time $\tau = 2 \times 10^{-23}$ s was assumed in order to obtain an upper limit for the effects of such a collision term. The evaluation of the Fourier transform of the current as well as the limits for the photon cross section are the same as before. The results are shown in fig. 4 by the long dashed line ($\vartheta_{\gamma} = 45°$). Within the numerical accuracy achieved they do not indicate a significant enhancement of the photon yield due to collective bremsstrahlung.

How can we understand the latter result? First of all we have to note that the photons emerge from the space- and time-variation of the nuclear current (3.6) [cf. eqs. (3.3) and (3.4)] which for finite systems does not reflect the actual stopping of nucleons. Indeed, we find a striking similarity in the space- and time-dependence of the collective current $j(r, t)$ as evaluated from TDHF and ETDHF [6]). In order to demonstrate the latter observation we show the relative velocity $\dot{R}(t)$ in fig. 5 for both cases, where the relative distance $R(t)$ is determined by the difference between the centers of masses at each time-step.
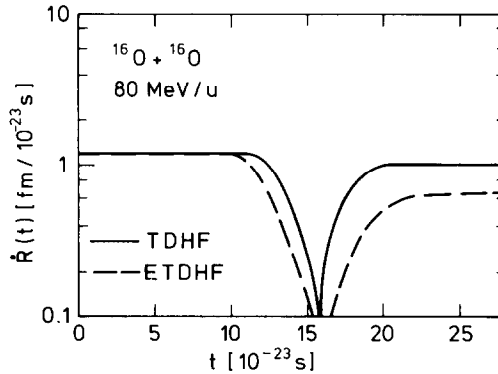

Fig. 5. Comparison of the relative velocity $\dot{R}(t)$ from TDHF and ETDHF calculations for $^{16}O + ^{16}O$ at 80 MeV/u.

Though in both cases the system $^{16}O + ^{16}O$ is transparent at 80 MeV/u, the time-dependence of $\dot{R}(t)$ appropriately reflects the average time variation of the nuclear current. We find that the decrease in the relative velocity (apart from a tiny

shift in time) is approximately the same for TDHF and ETDHF in the entrance channel. Relevant differences may only be found in the exit channel where the separation of the di-nuclear system is much slower in ETDHF.

The question remains, to what extent electromagnetic transitions between occupied and unoccupied time-dependent s.p. states, i.e. the second part of (2.9), contribute to the total photon yield.

The numerical technique is comparable to the one for the classical current described before except for the fact, that now in addition the spin current in eqs. (2.7) and (2.8) has to be evaluated and a large sum over $p–h$ matrix elements has to be performed. For an explorative study we restrict the summation over the unoccupied levels to those of the asymptotic s–d shell, while all occupied states of the s- and p-shell are taken into account. As has been checked in a single test run the latter restriction underestimates the total photon yield by roughly a factor of two.

The numerical results for the double differential γ-cross section are displayed in fig. 6 in terms of the full lines at 5°, 45° and 85°. The numerical error bars for the yield at 45° again are indicated by the vertical lines. Contrary to the collective bremsstrahlung contributions (cf. fig. 4) the photon yield is slightly enhanced at 90° in the c.m. system as compared to the more forward angles of 45° and 5°. The slope of the spectrum, furthermore, is flatter than that of the bremsstrahlung contribution and of the slab calculation and close to that of the experimental data for $^{12}C + ^{12}C$

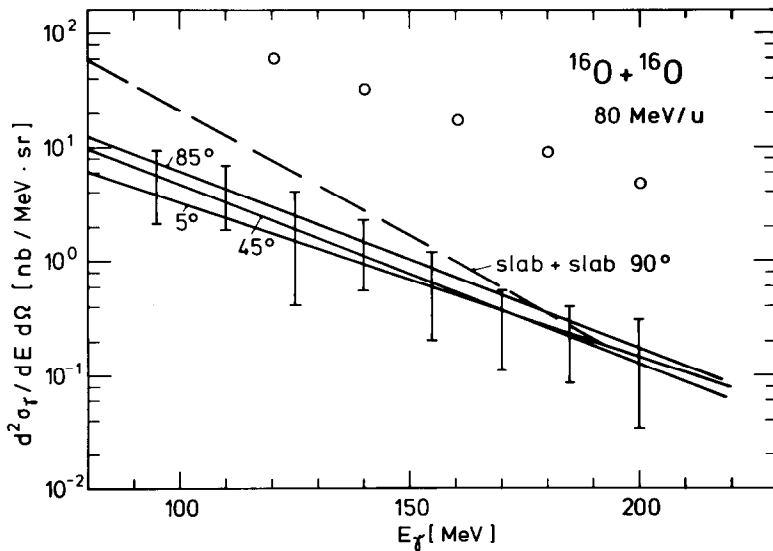Fig. 6. The energetic photon yield for $^{16}O + ^{16}O$ at 80 MeV/u as emerging from electromagnetic transitions between time-dependent s.p. states at $\vartheta_\gamma = 5°$, 45° and 85° in the c.m. system. The numerical uncertainty is demonstrated in terms of the vertical lines at $\vartheta_\gamma = 45°$. The long dashed line shows the corresponding result for $^{12}C + ^{12}C$ at 84 MeV/u and $\vartheta_\gamma = 90°$ in slab geometry (cf. fig. 1). Experimental data for $^{12}C + ^{12}C$ at 84 MeV/u and 90° are displayed in terms of the open circles [from ref. [11])].

at 84 MeV/u and 90° (open circles in fig. 6). Nevertheless, the absolute yields are again missed by more than an order of magnitude.

Summing up the contributions of collective bremsstrahlung (fig. 4) and electromagnetic transitions (fig. 6) for the higher γ-energies the minimum in the angular distribution at 90° disappears, but the sum accounts at most for 10% of the measured cross section [11].

4. Summary

We have studied high energy γ-ray emission in heavy-ion collisions from 80 MeV/u to 160 MeV/u in a microscopic framework, which allows to treat the collective stopping of the two nuclei by the common mean field, includes the correct energy-momentum relation of the nucleons via time-dependent s.p. states, takes care of distortions in coordinate and momentum space and includes the Pauli principle exactly. The extensive calculations performed allow for the following conclusions:

(i) The energetic photon yield due to collective bremsstrahlung is dominated by a quadrupole type angular distribution and underestimates the experimental cross section by about a factor of 20 at 80 MeV/u (cf. fig. 4). This observation also holds if the effects of residual nucleon–nucleon collisions on the collective current are taken into account.

(ii) Energetic photons due to electromagnetic transitions between time-dependent s.p. states show a characteristic dipole angular distribution in the c.m. system which flattens out in forward (backward) direction for very energetic photons in line with an increasing contribution from the nuclear spin current (cf. fig. 2). The slope of the energy distributions is in good agreement with experimental data in case of unrestricted three-dimensional calculations, whereas the total yield again is underestimated by more than one order of magnitude (cf. fig. 6).

(iii) The angle integrated differential cross sections follow approximately a power law of the type (3.1) as a function of the bombarding energy per nucleon in rough agreement with experimental data [12].

The question remains with respect to the missing 90% of the experimental cross sections. In our general formulation (sect. 2) we expect this yield to arise from two-particle contributions to the current operator in eq. (2.4), which are related with two-body vertices and exchange currents, but have not been considered in the present work. A similar experience has been gained with respect to pion production which appears to be dominated by two-body processes [7]. In more classical terms, proton–neutron bremsstrahlung [15] should contribute significantly to the experimental yield. A field theoretical treatment of these phenomena is in progress [16].

References

1) E.M. Nyman, Phys. Lett. **136B** (1984) 143
2) D. Vasak, W. Greiner, B. Müller, T. Stahl and M. Uhlig, Nucl. Phys. **A428** (1984) 291c
3) C.M. Ko, G. Bertsch and J. Aichelin, Phys. Rev. **C31** (1985) 2324
4) R. Shyam and J. Knoll, Nucl. Phys. **A448** (1986) 322
5) H. Nifenecker and J.P. Bondorf, Nucl. Phys. **A442** (1985) 478
6) M. Tohyama, Phys. Lett, **144B** (1984) 169; Nucl. Phys. **A437** (1985) 443
7) M. Tohyama, R. Kaps, D. Masak and U. Mosel, Phys. Lett. **136B** (1984) 226; Nucl. Phys. **A437** (1985) 739
8) W. Gordon, Z. Phys. **50** (1930) 630
9) P. Bonche, S. Koonin and J.W. Negele, Phys. Rev. **C13** (1976) 1226
10) W. Bauer, Diploma thesis, University of Giessen 1985 (unpublished)
11) E. Grosse *et al.*, submitted to Europhysics Letters
12) H. Noll, GSI-Report 85-9
13) R.Y. Cusson, R.K. Smith and J.A. Maruhn, Phys. Rev. Lett. **36** (1976) 1166;
    R.Y. Cusson, J.A. Maruhn and A.W. Meldner, Phys. Rev. **C18** (1978) 2589;
    R.Y. Cusson and A.W. Meldner, Phys. Rev. Lett. **42** (1979) 694
14) J.D. Jackson, Classical electrodynamics (Wiley, New York, 1962)
15) P.F.M. Koehler, K.W. Rothe and E.H. Thorndike, Phys. Rev. Lett. **18** (1967) 933
16) W. Bauer, T. Biro, W. Cassing, U. Mosel and M. Tohyama, in preparation